

Toward Support-free 3D Printing: A skeletal Approach for Partitioning Models

1017

Abstract

We propose an algorithm for partitioning a 3D model into the least number of parts for 3D printing without using any support structure. Minimizing support structures is crucial in reducing 3D printing material and time, partition-based methods are efficient means in realizing this objective. However, any partition will inevitably induce seams and cracks on the assembled model, which affects the aesthetics and strength of the finished surface. To achieve support-free fabrication while minimizing the effect of the seams, we put forward an optimization system with the minimization of the number of partitioned components and the total length of the cuts, under the constraints of support-free printing angle. We show that the optimization problem is NP-hard and propose a Monte Carlo method based on training-and-learning data to find an optimal solution to the objectives. We applied our partition method on a number of various 3D models. Finally, we validate our method by carrying out a serial of 3D printing experiments.

Categories and Subject Descriptors (according to ACM CCS): I.3.3 [Computer Graphics]: Picture/Image Generation—Line and curve generation

1. Introduction

3D printing, or additive manufacturing, has drawn growing interests from researchers in computer graphics. Fused deposition modeling (FDM), stereolithographic (SLA), Selective Laser Melting (SLM) and Selective Laser Sintering (SLS) and the four most popular means of 3D printing techniques. Although 3D printing has seen its applications in producing arbitrarily intricate 3D models, the price of the printing materials, especially for those with high quality, are still outrageously high. Therefore, it is desirable to reduce materials used in the fabrication process. Note that this is also a critical operation for reducing production time and therefore the total production cost. For this purpose, an efficient method is to minimize the support structures, which are removed in the post-processing phase of the fabrication task.

As for minimizing support structures, Autodesk R MeshMixer™ provides a semiautomatic orientation optimization tool to minimize support volume, support area, structural strength, or a combination of these three attributes. However, it requires professional experience in setting the geometric parameters manually. A number of literatures have studied various factors that influence the volume of supports, e.g., optimizing the topology of the support structure [DHL14, VGB14a], determining an optimal fabrication direction [ZLP*15, HBA13, PD11], partitioning any given model into a set of separate parts that satisfy particular geometric properties such as being pyramidal [HLZCO], has minimal packing volume [VGB*14b] or inter-lockable [SFLF15]. However, the partition results of these methods do not simultaneously respect the geometric properties and the support-free printability of the portioned

parts. Further, no existing methods ever consider the problem of partitioning a boundary-represented mesh into the least number of parts whose fabrication is free of support structures. The least number of portioned parts corresponds to the least number of seams on the final assembled model, which ensures a nice aesthetics preservation of the model surface; and the support-free fabrication saves material to the most extent, which is particularly helpful in printing objects made of metal powder, resin, or nice plastics, etc.

This paper addresses the problem of decomposing a 3D model into the least number of parts, each of which, when printed in a proper direction, is free of support materials. Unfortunately, this problem is identical to the multi-container packing problem, which has been shown to be NP-hard [FK07]. Our solution of the problem draws inspiration from the 1D representation of organic models, i.e., skeletons: the topology variations of a natural model can be well-encoded by its skeleton, and a segment of the skeleton corresponding to a chunk of a mesh; further, the mesh chunk is typically a cylinder-like shape which can be printed free of support structures if the printing direction is parallel to the skeletal direction.

We restrict our focus on organic or man-made models since those shapes merit well-defined skeletons. Further, support structures are required for the interior and exterior surface of a mesh model during the 3D printing process. Our approach assumes that the interior of a mesh model is hollowed and the mesh model is shelled with a printer-friendly thickness. Therefore, our objective is to partition a model according to the growth of its skeleton into a set of sub-parts, such that each sub-part is represented by a skeletal subgraph which can be fabricated in a good printing direction without any

support structure. In the meanwhile, we also look for a best set of partitioned subparts which induce the minimal partition length.

Formally, given a printing direction, if the angle formed by the normal of a facet and the printing direction is greater than or equal to θ which is a printer-dependent value (60° for a typical FDM printer), then the facet can be printed without using any support structure. This inspires us to compute a minimum set of subgraph of the skeleton, such that each edge in any subgraph subtends to an axis (the printing direction) by an angle of no larger than $\pi/2 - \theta$, the corresponding chunk of the mesh is therefore support-free as printed along this axis. In general, a cone of axes satisfies this angle constraint. However, the volume of the chunk should be within the working space of the printer. Further, if the center of mass of the chunk diverts from the support center too much, e.g., the gravitational torque applied at the mass center is too far away from the center of support that it bends the printing model by a layer of thickness, then the surface quality of the model is poor or the printing task fails since the next printing layer cannot be firmly attached to the previous layer. Our method handles all these issues in a unified Monte Carlo framework which simultaneously looks for the best set of subgraphs which is support-free and with minimal partition length while guaranteeing the extracted subgraphs to have the desired gravitational properties.

In short, our method makes the following contributions:

- We partition any given mesh model into the least number of parts that are printable free of support structures; meanwhile, we preserve the aesthetics of the surface with the least number of seams whose length is minimized.
- We propose a Monte Carlo graph partition method based on the guide of 1D Laplacian skeleton of a given mesh model, which simultaneously accounts for minimal partition length and gravitational constraints.

2. Related Work

3D Printing. As cutting-edge 3D printing devices continue to emerge, various 3D printing techniques start to evolve. In computer graphics, a number of literatures have focused on the fabrication of 3D models using 3D printers. Optimization works have been devoted to structural designs with emphasis on saving printing materials while preserving certain strength [SVB*12, ZPZ13, WWY*13, US13, LSZ*14]. The modeling of some particular features have also been studied, for example, deformation behavior [STC*13], animated mechanical characters [CTN*13, CLM*13], articulated models with mobile joints [BBJP12, CCA*12], models spinnable motions [BWBS14], and self-balancing [PWLS13].

Model Partition for 3D Printing. A 3D printer cannot directly print a model whose size is larger than the printer's working space. To overcome this practical limitation, Luo et al. [LBRM12] proposed a solution to partition a given 3D model into parts for 3D printing and then assemble the parts together. This approach has a few advantages: (i) it is cost-effective in the sense that we only need to print a replacement part for a corresponding broken part; (ii) it is convenient for storage and transportation; (iii) changing some parts of a model allows innovative designs. Along this line

of research, Hao et al. [HFW11] partitioned a large complex model into simpler 3D printable parts by using curvature-based partitioning. Hildebrand et al. [HBA13] addressed the directional bias issue in 3D printing by segmenting a 3D model into a few parts each of which is assigned an optimal printing orientation. Vanek et al. [VGB*14b] reduced the time and material cost of 3D printing by hollowing a 3D model into shells and breaking them into parts, a number of parameters including the total connecting area and volume of each segment are considered during the optimization process. Song et al. [SFLF15] recently developed a novel voxelization-based approach to construct inter-locking 3D parts from a given 3D model. Without using any glue, Xin et al. [XLF*11] and Song et al. [SFC12] take a 3D interlocking approach to construct and connect printed 3D parts to form an object assembly. Hu et al. [HLZCO] proposed an nice algorithm for decomposing a solid model into the least number of pyramids. However, their algorithm is only workable for volumetric models.

Shape Decomposition. In geometry processing, decomposing a shape into parts is a fundamental problem. Many research efforts have been devoted to the problem of model decomposition. An excellent survey can be found in [Sha08]. A large body of research are focusing on partitioning a given 3D model into meaningful parts which agree with human perception [KT03, KLT05, JLCW06, LZ07, GF08, CGF09, vKFK*14], among which geometric features captures shape concaveness are mostly exploited in accordance with the minima rules [HR84, HS97]. Other approaches are more application-oriented. For example, texture mapping techniques often require the input shape being decomposed into flat charts which can be flatten with image textures [ZSGS04, GP08]. Our method of partition are based on shape skeletons. While there have been previous work on skeleton based shape decomposition [LKA06, RT07, ATC*08], none of them are tailored towards support-free fabrication.

3. Overview

In nature, most organic models ubiquitously contain cylindrical parts [ZYH*15], e.g., arms, legs, etc. Moreover, an cylindrical part can be well represented by its corresponding 1D skeleton. Based on this property, a chunk of a mesh model can be fabricated free of support if its corresponding skeleton piece subtends to a printing direction by an angle of no large than θ , where θ is a printer-dependent threshold value determined by experiments. Hence, our problem naturally becomes partitioning a given 1D skeleton into sub-skeletons such that each sub-skeleton merits desirable printing properties including support-free and gravitational stable. In the remainder of the paper, by model we mean an organic mesh model of natural life form or articulated figures preserving nice topology features of real lives.

Choice of skeleton. Compared to natural skeletons, the medial axis can describe the topology of a mesh model more precisely [ZXW*15]. However, a medial axis of a 3D mesh model is a 2D surface which cannot be conveniently applied to describe the critical topology changes of the model. Additionally, the medial axis consists of intersecting pieces of planes and conic surfaces, presenting significant complications to algorithms that attempt to construct 3D medial axes. Reeb graph provides a possible choice for

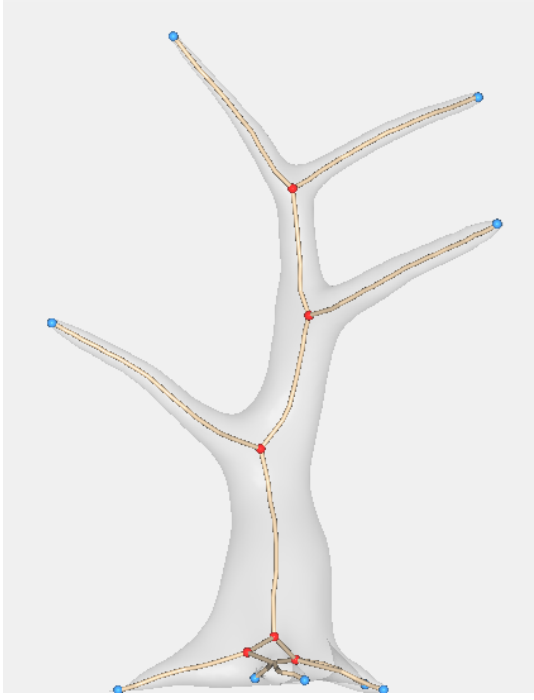


Figure 1: An illustration of a 3D mesh model and its 1D Laplacian skeleton.

1D skeleton. During the generation process of any reeb graph, the slicing direction and the position of the representative node on each slide (a connected region) seriously influence the choice of critical points and therefore generation of the Reeb graph. However, the determination of suitable slicing direction and representative nodes is an intractable problem. We resort to the 1D Laplacian skeleton proposed by [ATC*08] which is extracted by shrinking the mesh model using Laplacian smoothing, such 1D Laplacian skeleton provides an excellent choice for reasonably describing the geometrical and topological variations of any 3D model [ATC*08]. Figure 1 shows an example of the Laplacian skeleton.

Problem Statement. Our goal is hence to decompose the 1D Laplacian skeleton of the model into the least support-free subgraphs leads to a partition of the model into the least printable parts free of support structures and cracks on the final assembly model. In addition, since support structures result in bumpy supported areas, support-free fabrication also means a nice preservation of the surface quality of the parts. Further, a minimization of the number of cuts and the total cutting length means a minimum amount of seams and their lengths on the assembled model. Therefore, we focus on these two problems in this paper.

Unfortunately, finding such a decomposition is a non-trivial task. Consider a simple example of 1D Laplacian skeleton that is a fork with n vectors sharing a common origin; our objective is partitioning the fork into the least number of sub-forks such that each sub-fork can be packed into a cone of angle 2θ in order to make the sub-fork support-free when fabricated in a given direction. This problem is exactly the problem of packing n items with weight-

s w_1, \dots, w_n into bins of capacity c such that all items are packed into the fewest number of bins, which has been shown to be NP-hard [FK07].

we formulate the partition problem with both the objectives of the total number of cuts and the cutting length, under the constraint of printing angle of each branch with respect to the build platform, the angle between a cut plane and the printing direction, the dimension of each printed model with respect to the printable volume of a given printer, and the base area of a printed model. Since the problem is NP-hard, we propose a randomized Monte Carlo method in compliance with a set of carefully designed selection strategy to seek a practical solution to the optimization problem.

4. Algorithm

Let M denote the mesh model, and let S denote the Laplacian skeleton. We propose an algorithm for partitioning S into a minimum set of nice (disjoint) subgraphs, each of which can be fabricated in a 3D printer without using support structures. Decomposing S into two pieces can be done by duplicating a node v and splitting the arcs incident to v properly; however, decomposing M around v requires the determination of the position and normal of a cutting plane; to realize these and guarantee a nice look on the finished surface with shortest seams, we set a constraint of minimizing the peripheral length of a cut. For realizing the objectives, in addition to the angle constraint for the arcs, we need to consider the dimension constraint: the dimension of the printing model should be within the working space of a given 3D printer.

To summarize, our objectives are the minimization of (1) the number of partitioned components N ; (2) the total peripheral length of each cut L_i , i.e., $\sum L_i$.

The constraints of the problem are as follows: (1) Each arc of the partitioned subgraph subtends to an axis by an angle of no larger than θ , where θ is defined based on printing experiments without using any support structure. This guarantees that the corresponding mesh component is support-free during the printing process. (2) Let the normal direction of the cut c (pointing to the exterior of the partitioned part) be denoted as $n(c)$; as the directed arcs of H_i are translated to a common origin, they form a fork, the fork has a central ray, which is the middle axis of the minimum cone that encloses the fork, let $Cone(H_i)$ be the cone, let the central ray of $Cone(H_i)$ be denoted as $r(H_i)$; in order to guarantee support-free fabrication for the boundary of the cut, the angle between $n(c)$ and $r(H_i)$ should satisfy $A(n(c), r(H_i))\pi/2 + \theta$. (3) The base of a printing model should be large enough to gather sticky force from the building platform, such that the model is not deformed during the building process. Formally, let $b(H_i)$ denote the area of the base of the mesh component corresponding to H_i , let τ be a user-defined threshold value., then we have $b(H_i) \geq \tau$. Here τ can be determined by some simple printing experiments. (4) Each cut partitions a single subgraph.

To summarize, we have the following optimization system:

Objective: $\min N$ and $\min \sum (L_i)$ (1) Subject to: $A(e, r(H_i))\theta$, for each $e \in H_i$ (2) $A(n(c), r(H_i)) \leq \pi/2 + \theta$ (3) $b(H_i) \geq \tau$ (4) $c \cap S = c \cap H_i$ (5) where H_i is the target subgraph to be cut off.

Assume that we are given a function $TirmBFS(v, G)$ which traverses G from v in a breath first search manner until all arcs satisfying constraints (2-3) are determined, we have the following algorithm for skeleton decomposition. The main idea of our algorithm is to randomly search the graph using Monte Carlo Method, which randomly chooses a node of S to start traversing and randomly chooses an arc of the current node as the exit path.

Algorithm 1 Algorithm: *SkeletonMeshDecomposition*(S, M)

Input: The Laplacian skeleton S of a mesh model M ;

Output: The decomposition of S into a set of the least pieces of subgraphs T , each arc of which subtends to an axis by an angle of no larger than θ ;

```

1:  $T = \emptyset$ ;  $min = \inf$ ;  $count = 0$ ;  $max - iter$  = a user defined large constant;
2: while  $count < max - iter$  do
3:    $G = S$ ;  $U = \emptyset$ ;
4:   while  $G \neq \emptyset$  do
5:     for ( $i = 1$ ;  $i < |S|$ ;  $i++$ ) do
6:        $H = TirmBFS(v_i, S, \theta)$ ;
7:        $H = S/H$ ;
8:        $U = U \cup H$ ;
9:       if  $|U| < min$  then
10:         $T = U$ ;
11:         $min = |U|$ ;
12:       end if
13:     end for
14:   end while
15:    $count = count + 1$ ;
16: end while
17: return  $T$ ;
```

Skeleton Partition: Next we shall show how $TirmBFS(v, S, \theta)$ works to find a maximal subgraph starting at v that satisfies the angle constraint. Let H be the current subgraph obtained. When an arc e of G is visited, we need to determine whether it should be included into H . If the start of each outgoing arc of H is moved to a common site, then the arcs form a fork (Figure 2). A naive method to judge whether e should be included is to move the start of e to the origin of the fork, and compute the angle between e and each arc of the fork, e is included if the maximum angle between e and each arc of the fork does not exceed 0.5π . However, this method would require $O(K^2)$ time, where K is the number of the nodes of S . To speed up this process, we keep the pair of vectors that form the largest angle and judge whether a new vector expands the mouth of the fork; if so, determine the other vector (may not be an arc of H). See Figure 2, let \hat{e}_i and \hat{e}_j be the units of these two vectors obtained so far. For simplicity, we denoted by $F(\hat{e}_i, \hat{e}_j)$ the fork with the starts of all unit vectors converging at the origin of the coordinate frame, where \hat{e}_i and \hat{e}_j are the pair of unit vectors that form the largest angle in the fork. Let \hat{e}_k be the unit of a new vector to be processed next, if \hat{e}_k penetrates through the blue circle, then no change need to be made to the fork; otherwise, let $D_{i,j}$ denote the spherical disk that passes through the endpoints of \hat{e}_i and \hat{e}_j whose central axis is collinear with $\hat{e}_i + \hat{e}_j$, let $c_{i,j}$ be the center of $D_{i,j}$, let $B_{i,j}$ be the boundary circle of $D_{i,j}$. The circle passing through \hat{e}_k and $c_{i,j}$, denoted as $O(\hat{e}_k, c_{i,j})$, intersects $B_{i,j}$ at two points, let q the

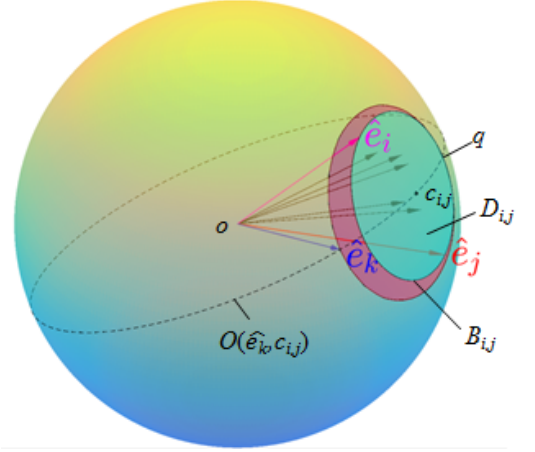


Figure 2: Illustration of unit vectors, unit sphere, spherical disks, and the determination of taking a new edge in *TrimBFS*.

point further away from the endpoint of \hat{e}_k , then \vec{oq} and \hat{e}_k are the two extreme vectors that to be used in the next iteration. To summarize, A new arc e_k is taken by Function *TirmBFS* if and only if one of the following two conditions is met: (1) the angle between \vec{oq} and \hat{e}_k , denoted as $A(\vec{oq}, \hat{e}_k)$, satisfies $A(\vec{oq}, \hat{e}_k) \leq A(\vec{oq}, \hat{e}_i)$; (2) $A(\vec{oq}, \hat{e}_k) \leq \pi - 2\theta$, where $q = O(\hat{e}_k, c_{i,j}) \cap B_{i,j}$.

Mesh Partition:

[Anton: Optimization of cutting sequence]

Although the skeleton partition tells us a rough sketch of the mesh partition, i.e., the cutting plane should be in the vicinity of each node v incident to two distinct subgraphs. Yet we need to determine the exact positions of the cutting planes. For each node v that is incident to at least two distinct subgraphs H_i and H_j , we process it using the following cutting principle:

The Cutting Scheme for M : See Figure 3, at the position of node v , define two fillets each of which contains all planes that orthogonal to the vectors in $Cone(H_i)$ or $Cone(H_j)$, let $Fillet(H_i)$ and $Fillet(H_j)$ be the two fillets respectively. Depending on the relative position of $Fillet(H_i)$ and $Fillet(H_j)$, we have the following cases:

$$Fillet(H_i) \cap Fillet(H_j) / v \neq \emptyset$$

See Figure 3(a) for an illustration of the case. To address the issue, we shall randomly sample a set of cutting planes from $Fillet(H_i) \cap Fillet(H_j) / v$, and determine the one achieving the minimum cutting length.

$$Fillet(H_i) \cap Fillet(H_j) = v$$

See Figure 3(b). In this case, two cuts c_1 and c_2 are inevitable in order to separate the mesh, however, care must be taken as the angle between c_1 and c_2 should be constrained by $A(n(c_1), n(c_2)) \leq \pi/2 + \theta$. If this constraint is violated, one more cut in between c_1 and c_2 is required; while the base of each partitioned component should be constrained by $b(H_i) \geq \tau$ and $b(H_j) \geq \tau$. If any of the constraints is not satisfied, we shall translate the fillets along the build direction in an opposite sense until the constraints are satisfied (See Figure fillets). In this process, if the translation hits an

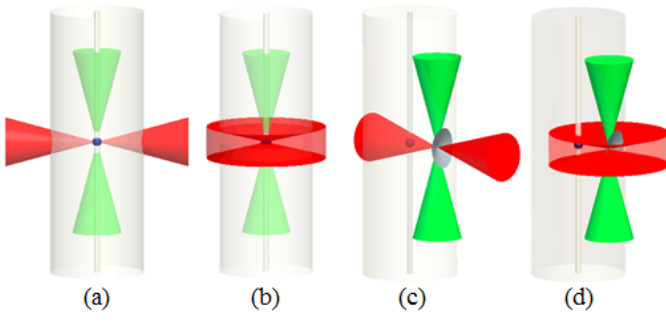


Figure 3: Illustration of fillets: (a) two fillets with their apexes coinciding at a node of S share an intersection zone; (b) two fillets with their apexes coinciding at a node of S share a single point; (c) two fillets with their apexes coinciding at a concave vertex of R_v share an intersection zone; (d) two fillets with their apexes coinciding at a concave vertex of R_v share the concave vertex only. The two fillets are marked by red and green colors respectively.

Let $R(v)$ be the set of concave vertices on M that are incident to v during the Laplacian shrinking process, we shall truncate $R(v)$ such that the non-significant concave vertices are removed away. Here, given a vertex v_i and any of its neighbor v_j , v_i is concave if $(v_i - v_j)(n_j - n_i)$ is nonnegative, the significance of a concave vertex can be quantified as the magnitude of $(v_i - v_j)(n_j - n_i)$ [AZC*12]. See Figure 3(c-d), for each vertex in $R(v)$, we shall process a pair of fillets as done for node v above. Particularly, if v is neighbor to at least three nodes in S while is only neighbored to a single node w in subgraph H_i , then the separation of the mesh component corresponding to H_i may not be feasible if only $R(v)$ is used, this is because the position of v is designed for the purpose of connecting the different branches. To separate the mesh component of H_i , we process arc vw as follows: Given a user-defined threshold value δ , if $|vw| \leq \delta$, then $R(v)$ is extended to contain the concave vertices of M that are incident to w . On the other hand, if $|vw| > \delta$, then a partition of the arc vw by an interval of δ is applied. Subsequently, for each node along the arc vw , the above scheme for processing a pair of fillets for node v is exploited, see Figure 4. Finally, if the cut-subgraph constraint (Eq. (5)) is violated, a sequence of iterative cutting is required.

However, a split of the 1D skeleton cannot tell us the exact position of the cut on the mesh. Sometimes, it is possible for a piece of meat, i.e., a mesh component, that is not printable free of support even though its corresponding skeleton is printable free of support. This is because the skeleton piece that shares a junction node with any other subgraph may compromise its topology locally [ATC*08], and therefore cannot precisely describe the local topology feature of the partitioned meat. In this case, we shall regenerate the skeleton of the meat by running our skeleton partition algorithm on the meat, and then apply the *SkeletonMeshDecomposition* Algorithm on it. Refer to Figure 5 for an illustration.

Cut-subgraph Intersection Detection: In order to take care of Eq. (7), the intersections of a cut and the subgraphs can be efficiently

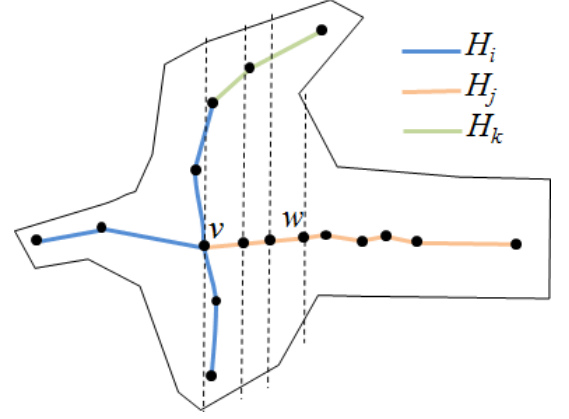


Figure 4: 2D illustration editing a long arc for cutting.

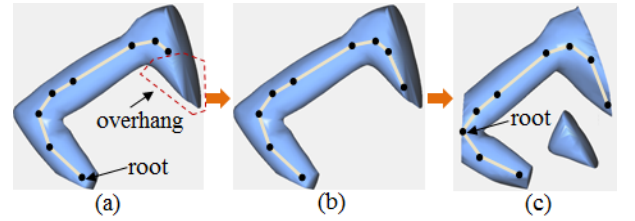


Figure 5: Illustration of editing the mesh component of a printable subgraph: (a) A meat with an overhang that requires support; (b) Regeneration of the skeleton of the meat by *SkeletonMeshDecomposition* Algorithm; (c) the partition result by *SkeletonMeshDecomposition* Algorithm.

determined by taking advantage of the correspondence between the mesh vertices and the skeleton nodes: each vertex of M is mapped to a single node of S . Therefore, as a cut goes through the mesh surface, the endpoints of the cut edges of M lend us the information of the cut subgraphs. Approximately, if a cut c goes into an edge whose endpoints are incident to a subgraph H , then c cuts H .

In line 2 of *TrimBFS*, the BFS process randomly chooses an arc incident to v to proceed on. In order to guarantee a greater chance of converging to the optimal result in a short time, we apply a training-and-learning procedure for the first 1000 runs. Formally, let N_v be the number of times an arc is chosen as the exit arc when node v is visited. Given the data of the first 1000 runs, as a node v is visited, the probability of choosing an arc e as an outgoing arc in the subsequent runs is,

$$P(v, e) = N_v / 1000 \quad (7)$$

To further speed up the process of *Trim-BFS*, we assign a mark that stores the minimum number of subgraphs obtained so far, such that the current branching can be terminated if its output number of subgraphs is larger than the mark.

Since the traversing process assigns a specific direction to each arc that was originally undirected in S , it is not obvious whether the angle constraint is satisfied. To clarify this, we provide the following lemma.

Algorithm 2 Algorithm: *TrimBFS*(v, S, θ)

Input: A node v of Laplacian skeleton S , an angular value θ ;
Output: A maximal subgraph H rooted at v and its corresponding mesh component that meet the constraints (Eq.2-5);

- 1: starting from v , initialize $F(\hat{e}_i, \hat{e}_j); H = \emptyset$;
- 2: **while** the current arc e_k of S picked by the BFS process is nonempty **do**
- 3: **if** $A(\overrightarrow{oc_{i,j}}, \hat{e}_k) \leq A(\overrightarrow{oc_{i,j}}, \hat{e}_i)$ **then**
- 4: $H = H \cup e_k$;
- 5: **end if**
- 6: $q = O(\hat{e}_k, c_{i,j}) \cap B_{i,j}$;
- 7: **if** $A(\overrightarrow{dq}, \hat{e}_k) \leq \pi - 2\theta$ **then**
- 8: $\hat{e}_i = \hat{e}_k$;
- 9: $\hat{e}_j = \overrightarrow{dq}$;
- 10: update $B_{i,j}$ and $c_{i,j}$;
- 11: $H = H \cup e_k$;
- 12: **end if**
- 13: **end while**
- 14: call the cutting scheme for M ;
- 15: $M = M/M_H$;
- 16: **return** H and M_H ;

Lemma 1: $H = \text{TrimBFS}(v, G, \theta)$ is a maximal subgraph of G that satisfies the angle constraint, i.e., each arc of H subtends to an axis by an angle of no larger than θ .

Proof: Suppose to the contrary that H violates the angle constraint, there exists a directed arc that does not satisfy the angle constraint. For example, arc $\vec{a} \rightarrow (c, a)$ or arc $\vec{a} \rightarrow (b, c)$ in Figure 6. Such case is impossible as Line 3 and Line 6 of function *Trim-BFS* excludes any directed arc that violates the angle constraint of no larger than θ with respect to the (virtual) central axis. It remains to prove that H is maximal, i.e., the largest graph rooted at v that covers all the arcs that satisfies the angle constraint. Suppose that this is not true, there must exist an arc that was mistakenly discarded due to the direction in which the arc is traversed. Let (b, c) be one of such arcs, as illustrated in Figure 6(a). When the arc is directed from b to c , it is not included as it violates the angle constraint, but can be included if the arc directed from c to b . We shall prove in a case-by-case basis. If c is not reachable from v via a directed path passing through b (Figure 6(c)), then c is only reachable from b , arc bc should not be included and line 6 of Function *Trim-BFS* correctly handle this case. Otherwise, c is reachable from v via a directed path without passing through b (Figure 6(d)). As c is visited, by Line 2 of Function *Trim-BFS*, each arc leaving c is considered, and $\vec{a} \rightarrow (c, b)$ is correctly included into H . This completes the proof. \square

Figure WSX:

5. Results

[In the examples, show how the training-and-learning procedure saves running time]

We have evaluated our skeletal partition approach on a number of models, including man-made art objects and organic forms. Fig-

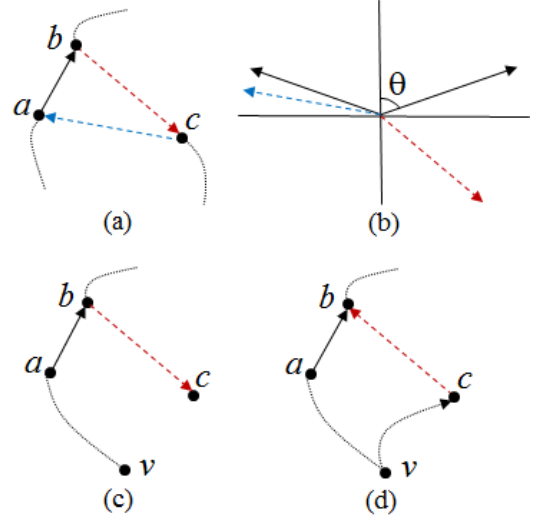


Figure 6: Illustration of taking a directed arc into a maximal subgraph by *Trim-BFS*.

ures LLL show partition results, and the printed models and their experimental statistics.

[show the printed model without any cutting operation, the partitioned CAD model, the assembled printed model, the statistics on time and material saving, for all 12 models]

6. Conclusion, Limitation, and Future Work

Compared with existing partition-based methods, the advantages of our partition method are as follows:

- The models are support-free, especially for the 3D printing techniques including SLA, SLM and SLS. For FDM technique, it requires a bed of support that consumes very little volume of materials.
- The seams on the assembled model are minimized in terms of cut number and cut length.

References

- [ATC*08] AU O. K., TAI C., CHU H., COHEN-OR D., LEE T.: Skeleton extraction by mesh contraction. *ACM Trans. Graph.* 27, 3 (2008). URL: <http://doi.acm.org/10.1145/1360612.1360643>, doi:10.1145/1360612.1360643. 2, 3, 5
- [AZC*12] AU O. K.-C., ZHENG Y., CHEN M., XU P., TAI C.-L.: Mesh segmentation with concavity-aware fields. *Visualization and Computer Graphics, IEEE Transactions on* 18, 7 (2012), 1125–1134. 5
- [BBJP12] BÄCHER M., BICKEL B., JAMES D. L., PFISTER H.: Fabricating articulated characters from skinned meshes. *ACM Trans. Graph.* 31, 4 (2012), 47:1–47:9. URL: <http://doi.acm.org/10.1145/2185520.2185543>, doi:10.1145/2185520.2185543. 2
- [BWBS14] BÄCHER M., WHITING E., BICKEL B., SORKINE-HORNUNG O.: Spin-it: optimizing moment of inertia for spinnable objects. *ACM Trans. Graph.* 33, 4 (2014), 96:1–96:10. URL: <http://doi.acm.org/10.1145/2601097.2601157>, doi:10.1145/2601097.2601157. 2

- [CCA*12] CALÌ J., CALIAN D. A., AMATI C., KLEINBERGER R., STEED A., KAUTZ J., WEYRICH T.: 3d-printing of non-assembly, articulated models. *ACM Trans. Graph.* 31, 6 (2012), 130. URL: <http://doi.acm.org/10.1145/2366145.2366149>, doi:10.1145/2366145.2366149. 2
- [CGF09] CHEN X., GOLOVINSKIY A., FUNKHOUSER T. A.: A benchmark for 3d mesh segmentation. *ACM Trans. Graph.* 28, 3 (2009). 2
- [CLM*13] CEYLAN D., LI W., MITRA N. J., AGRAWALA M., PAULY M.: Designing and fabricating mechanical automata from mocap sequences. *ACM Trans. Graph.* 32, 6 (2013), 186:1–186:11. URL: <http://doi.acm.org/10.1145/2508363.2508400>, doi:10.1145/2508363.2508400. 2
- [CTN*13] COROS S., THOMASZEWSKI B., NORIS G., SUEDA S., FORBERG M., SUMNER R. W., MATUSIK W., BICKEL B.: Computational design of mechanical characters. *ACM Trans. Graph.* 32, 4 (2013), 83:1–83:12. URL: <http://doi.acm.org/10.1145/2461912.2461953>, doi:10.1145/2461912.2461953. 2
- [DHL14] DUMAS J., HERGEL J., LEFEBVRE S.: Bridging the gap: automated steady scaffolds for 3d printing. *ACM Trans. Graph.* 33, 4 (2014), 98:1–98:10. URL: <http://doi.acm.org/10.1145/2601097.2601153>, doi:10.1145/2601097.2601153. 1
- [FK07] FUKUNAGA A. S., KORF R. E.: Bin completion algorithms for multicontainer packing, knapsack, and covering problems. *J. Artif. Int. Res.* 28, 1 (Mar. 2007), 393–429. URL: <http://dl.acm.org/citation.cfm?id=1622591.1622602>. 1, 3
- [GF08] GOLOVINSKIY A., FUNKHOUSER T.: Randomized cuts for 3D mesh analysis. *ACM Transactions on Graphics (Proc. SIGGRAPH ASIA)* 27, 5 (Dec. 2008). 2
- [GP08] GARCÍA I., PATOW G.: Igt: inverse geometric textures. *ACM Trans. Graph.* 27 (December 2008), 137:1–137:9. 2
- [HBA13] HILDEBRAND K., BICKEL B., ALEXA M.: Orthogonal slicing for additive manufacturing. *Computers & Graphics* 37, 6 (2013), 669–675. URL: <http://dx.doi.org/10.1016/j.cag.2013.05.011>, doi:10.1016/j.cag.2013.05.011. 1, 2
- [HFW11] HAO J., FANG L., WILLIAMS R. E.: An efficient curvature-based partitioning of large-scale stl models. *Rapid Prototyping Journal* 17, 2 (2011), 116–127. 2
- [HLZCO] HU R., LI H., ZHANG H., COHEN-OR D.: Approximate pyramidal shape decomposition. 1, 2
- [HR84] HOFFMAN D. D., RICHARDS W. A.: Parts of recognition. *Cognition* 18, 1 (1984), 65–96. 2
- [HS97] HOFFMAN D. D., SINGH M.: Saliency of visual parts. *Cognition* 63, 1 (1997), 29–78. 2
- [JLCW06] JI Z., LIU L., CHEN Z., WANG G.: Easy mesh cutting. *Comput. Graph. Forum* 25, 3 (2006), 283–291. 2
- [KLT05] KATZ S., LEIFMAN G., TAL A.: Mesh segmentation using feature point and core extraction. *The Visual Computer* 21, 8–10 (2005), 649–658. 2
- [KT03] KATZ S., TAL A.: Hierarchical mesh decomposition using fuzzy clustering and cuts. *ACM Trans. Graph.* 22, 3 (2003), 954–961. 2
- [LBRM12] LUO L., BARAN I., RUSINKIEWICZ S., MATUSIK W.: Chopper: partitioning models into 3d-printable parts. *ACM Trans. Graph.* 31, 6 (2012), 129. URL: <http://doi.acm.org/10.1145/2366145.2366148>, doi:10.1145/2366145.2366148. 2
- [LKA06] LIEN J.-M., KEYSER J., AMATO N. M.: Simultaneous shape decomposition and skeletonization. In *Proceedings of the 2006 ACM symposium on Solid and physical modeling* (2006), ACM, pp. 219–228. 2
- [LSZ*14] LU L., SHARF A., ZHAO H., WEI Y., FAN Q., CHEN X., SAVOYE Y., TU C., COHEN-OR D., CHEN B.: Build-to-last: strength to weight 3d printed objects. *ACM Trans. Graph.* 33, 4 (2014), 97:1–97:10. URL: <http://doi.acm.org/10.1145/2601097.2601168>, doi:10.1145/2601097.2601168. 2
- [LZ07] LIU R., ZHANG H.: Mesh segmentation via spectral embedding and contour analysis. *Comput. Graph. Forum* 26, 3 (2007), 385–394. 2
- [PD11] PADHYE N., DEB K.: Multi-objective optimisation and multi-criteria decision making in sls using evolutionary approaches. *Rapid Prototyping Journal* 17, 6 (2011), 458–478. 1
- [PWLS13] PRÉVOST R., WHITING E., LEFEBVRE S., SORKINE-HORNUNG O.: Make it stand: balancing shapes for 3d fabrication. *ACM Trans. Graph.* 32, 4 (2013), 81:1–81:10. URL: <http://doi.acm.org/10.1145/2461912.2461957>, doi:10.1145/2461912.2461957. 2
- [RT07] RENIERS D., TELEA A.: Skeleton-based hierarchical shape segmentation. In *Shape Modeling and Applications, 2007. SMI'07. IEEE International Conference on* (2007), IEEE, pp. 179–188. 2
- [SFC12] SONG P., FU C., COHEN-OR D.: Recursive interlocking puzzles. *ACM Trans. Graph.* 31, 6 (2012), 128. URL: <http://doi.acm.org/10.1145/2366145.2366147>, doi:10.1145/2366145.2366147. 2
- [SFLF15] SONG P., FU Z., LIU L., FU C.: Printing 3d objects with interlocking parts. *Computer Aided Geometric Design* 35–36 (2015), 137–148. URL: <http://dx.doi.org/10.1016/j.cagd.2015.03.020>, doi:10.1016/j.cagd.2015.03.020. 1, 2
- [Sha08] SHAMIR A.: A survey on mesh segmentation techniques. *Comput. Graph. Forum* 27, 6 (2008), 1539–1556. 2
- [STC*13] SKOURAS M., THOMASZEWSKI B., COROS S., BICKEL B., GROSS M. H.: Computational design of actuated deformable characters. *ACM Trans. Graph.* 32, 4 (2013), 82:1–82:10. URL: <http://doi.acm.org/10.1145/2461912.2461979>, doi:10.1145/2461912.2461979. 2
- [SVB*12] STAVA O., VANEK J., BENES B., CARR N. A., MECH R.: Stress relief: improving structural strength of 3d printable objects. *ACM Trans. Graph.* 31, 4 (2012), 48:1–48:11. URL: <http://doi.acm.org/10.1145/2185520.2185544>, doi:10.1145/2185520.2185544. 2
- [US13] UMETANI N., SCHMIDT R.: Cross-sectional structural analysis for 3d printing optimization. In *SIGGRAPH Asia 2013 Technical Briefs* (2013), SA '13, pp. 5:1–5:4. 2
- [VGB14a] VANEK J., GALICIA J. A. G., BENES B.: Clever support: Efficient support structure generation for digital fabrication. *Comput. Graph. Forum* 33, 5 (2014), 117–125. URL: <http://dx.doi.org/10.1111/cgf.12437>, doi:10.1111/cgf.12437. 1
- [VGB*14b] VANEK J., GALICIA J. A. G., BENES B., MECH R., CARR N. A., STAVA O., MILLER G. S. P.: Packmerger: A 3d print volume optimizer. *Comput. Graph. Forum* 33, 6 (2014), 322–332. URL: <http://dx.doi.org/10.1111/cgf.12353>, doi:10.1111/cgf.12353. 1, 2
- [vKFK*14] VAN KAICK O., FISH N., KLEIMAN Y., ASAFI S., COHEN-OR D.: Shape segmentation by approximate convexity analysis. *ACM Trans. Graph.* 34, 1 (2014), 4:1–4:11. 2
- [WWY*13] WANG W., WANG T. Y., YANG Z., LIU L., TONG X., TONG W., DENG J., CHEN F., LIU X.: Cost-effective printing of 3d objects with skin-frame structures. *ACM Trans. Graph.* 32, 6 (2013), 177:1–177:10. URL: <http://doi.acm.org/10.1145/2508363.2508382>, doi:10.1145/2508363.2508382. 2
- [XLF*11] XIN S., LAI C., FU C., WONG T., HE Y., COHEN-OR D.: Making burr puzzles from 3d models. *ACM Trans. Graph.* 30, 4 (2011), 97. URL: <http://doi.acm.org/10.1145/2010324.1964992>, doi:10.1145/2010324.1964992. 2
- [ZLP*15] ZHANG X., LE X., PANOTOPOULOU A., WHITING E., WANG C. C. L.: Perceptual models of preference in 3d printing direction. *ACM Trans. Graph.* 34, 6 (2015), 215:1–215:12. 1
- [ZPZ13] ZHOU Q., PANETTA J., ZORIN D.: Worst-case structural analysis. *ACM Trans. Graph.* 32, 4 (2013), 137:1–137:12. URL: <http://doi.acm.org/10.1145/2461912.2461967>, doi:10.1145/2461912.2461967. 2

- [ZSGS04] ZHOU K., SYNDER J., GUO B., SHUM H.-Y.: Iso-charts: stretch-driven mesh parameterization using spectral analysis. In *Proceedings of the 2004 Eurographics/ACM SIGGRAPH symposium on Geometry processing* (2004), ACM, pp. 45–54. [2](#)
- [ZXW*15] ZHANG X., XIA Y., WANG J., YANG Z., TU C., WANG W.: Medial axis tree - an internal supporting structure for 3d printing. *Computer Aided Geometric Design* 35-36 (2015), 149–162. URL: <http://dx.doi.org/10.1016/j.cagd.2015.03.012>, doi:10.1016/j.cagd.2015.03.012. [2](#)
- [ZYH*15] ZHOU Y., YIN K., HUANG H., ZHANG H., GONG M., COHEN-OR D.: Generalized cylinder decomposition. *ACM Trans. Graph.* 34, 6 (Oct. 2015), 171:1–171:14. [2](#)



Figure 7: For publications with color tables (i.e., publications not offering color throughout the paper) please **observe**: for the printed version – and ONLY for the printed version – color figures have to be placed in the last page.

For the electronic version, which will be converted to PDF before making it available electronically, the color images should be embedded within the document. Optionally, other multimedia material may be attached to the electronic version.